are especially apparent for the dehydrated sample (Figure 4C), for which qualitative trends can be seen even without computer deconvolution. For that sample, the apparent spin diffusion efficiency between the two types of silanol protons implies that there are substantial dipolar interactions between these two spin sets. Although a true calculation of internuclear distances would require a detailed model of structure and dynamics at the surface, a crude estimate from these data indicates a mean distance between the hydrogen-bonded and isolated silanol protons of less than 10 Å.

Deconvolution of the results given in Figure 4B indicates that ^{1}H spin diffusion between the water protons and silanol protons is almost nonexistent on the microsecond-to-millisecond time scale of this experiment and that spin diffusion between the two types of silanol protons occurs with a rate that is comparable with that in the evacuated sample (Figure 4C). The combination of these results and those of the T_1 measurements implies that, for the untreated silica gel sample, ^{1}H spin diffusion between the physisorbed water and surface silanols occurs with a correlation time, τ_c, such that $1 \text{ s} > \tau_c > 15$ ms.

3. Comparisons with IR Results. The ^{1}H CRAMPS spectra reported here are consistent with the results from previous infrared spectroscopic studies of silica gel. McDonald[3] reported O–H stretching absorbances for physisorbed water, hydrogen-bonded SiOH groups, and isolated SiOH groups in the IR spectrum of fumed silica. Several different types of hydrogen-bonded silanols were observed in the IR spectra, consistent with the variety of coupled silanols observed in the ^{1}H CRAMPS spectra. In both the IR and CRAMPS spectra the physisorbed water peak disappears when the silica is evacuated at 25–30 °C. While most of the IR absorbance associated with the hydrogen-bonded silanols disappeared upon evacuation at 500 °C, a weak absorbance, which was assigned to weakly hydrogen-bonded silanols, remained. These weakly hydrogen-bonded silanols may not be resolved in the CRAMPS spectrum of the silica sample evacuated at 500 °C, or they may not be present in the study reported here, since the sample was evacuated for 16 h, in contrast to the 30-min evacuation used in the IR study.

The ^{1}H CRAMPS technique is a valuable complement to IR spectroscopy, since in NMR the observed area of a given peak is directly proportional to the number of protons giving rise to that peak, and a wide variety of NMR relaxation experiments can be used to study the geometrical arrangements and dynamics of protons on the silica surface.

Conclusions

The results of this study show that state-of-the-art ^{1}H CRAMPS NMR techniques, including various kinds of relaxation experiments, are capable not only of distinguishing structurally different types of hydroxyl moieties on a silica surface but also of addressing the issue of proximity of one type relative to the others. Two distinctly different types of silanol groups are identified, and it is found that the hydrogen-bonded types are the ones that are eliminated first by thermal dehydration. More detailed studies of this type, especially in conjunction with ^{29}Si MAS NMR and IR experiments, should greatly enhance the quality of knowledge in this area.

Acknowledgment. Support from National Science Foundation Grant CHE-8610151 and use of the Colorado State University Regional NMR Center, funded by National Science Foundation Grant CHE-8616437, are gratefully acknowledged.

Registry No. Silanol, 14475-38-8.

Catecholate LMCT Bands as Probes for the Active Sites of Nonheme Iron Oxygenases[1]

D. D. Cox,[†] S. J. Benkovic,[‡] L. M. Bloom,[‡] F. C. Bradley,[†] M. J. Nelson,[§] L. Que, Jr.,*[†] and D. E. Wallick[‡]

Contribution from the Department of Chemistry, University of Minnesota, Minneapolis, Minnesota 55455, Department of Chemistry, The Pennsylvania State University, University Park, Pennsylvania 16802, and Central Research and Development Department, E. I. du Pont de Nemours & Company, Wilmington, Delaware 19898. *Received July 3, 1987*

Abstract: A series of [Fe^{III}L(catecholate)] complexes has been synthesized to correlate the energies of catecholate-to-Fe(III) charge-transfer transitions with the nature of the iron coordination environment. L is a tetradentate tripodal ligand, $N(CH_2X)_3$, where X can be phenolate, carboxylate, pyridine, or benzimidazole, or a combination thereof, and the resulting ternary complexes are high-spin ferric based on their EPR spectra. The complexes exhibit two ligand-to-metal charge-transfer (LMCT) bands in the 400–900-nm spectral region; these are shown to be catecholate-to-Fe(III) charge transfer in nature by resonance Raman studies. The LMCT bands systematically shift to lower energy as oxyanionic ligands on the tripod are replaced by neutral nitrogen ligands, which is consistent with the increased Lewis acidity of the metal center. These observations have been used to gain insight into the iron coordination environment of rat liver phenylalanine hydroxylase and soybean lipoxygenase, both of which form catechol complexes in their Fe(III) forms. The catechol complexes of these enzymes exhibit spectral features that are similar to those of the synthetic catecholate complexes. Based on the energies of the observed catecholate LMCT bands, it is proposed that the iron sites in phenylalanine hydroxylase and lipoxygenase resemble that of the tripod with two pendant pyridines and one carboxylate. These observations should complement other approaches for deducing the metal coordination environment in oxygenases which lack a visible chromophore, i.e., ligand-field spectral studies which provide information on coordination number and geometry, and EPR studies with NO and ^{17}O-labeled ligands which provide information on the binding of exogenous ligands.

There has been recent growing interest in the active site structure of the nonheme iron oxygenases and how the coordination chemistry of the iron center relates to the enzymatic function.[2,3] Our understanding of the mechanism for oxygen activation by these enzymes is rudimentary compared to that for the heme-containing oxygenases because of the paucity of information regarding the nature of their active sites. Some of these enzymes, such as catechol 1,2-dioxygenase,[4] protocatechuate 3,4-di-

[†] University of Minnesota.
[‡] Pennsylvania State University.
[§] E. I. du Pont de Nemours.

(1) Contribution No. 4415 from the Central Research and Development Department, E. I. du Pont de Nemours & Co.
(2) Que, L., Jr. *Struct. Bonding (Berlin)* **1980**, *40*, 39–72.
(3) Que, L., Jr. *Adv. Inorg. Biochem.* **1983**, *5*, 166–199.

0002-7863/88/1510-2026$01.50/0

Scheme I

Tripodal Ligands

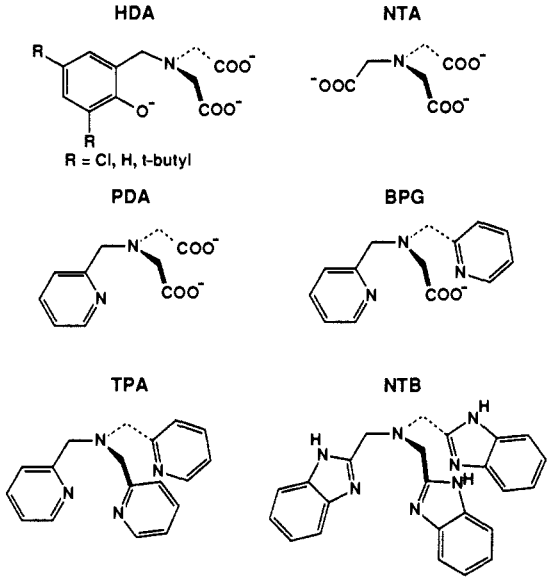

oxygenase,[5] and *p*-hydroxyphenylpyruvate dioxygenase,[6] have visible chromophores due to tyrosinate-to-Fe(III) charge-transfer transitions.[7] However, others such as protocatechuate 4,5-dioxygenase[8] and phenylalanine hydroxylase[9] are spectroscopically less accessible because the active site involves a ferrous center. Strategies are being developed to probe the coordination chemistry of ferrous sites. By studying Fe(II) ligand field bands in the CD and MCD spectrum, Whittaker and Solomon gained insight into the geometries of the iron sites in soybean lipoxygenase and superoxide dismutase.[10] Arciero and Lipscomb utilized the EPR properties of NO complexes of protocatechuate 4,5-dioxygenase together with ^{17}O-labeled ligands to determine the number of available exogenous binding sites.[11] In this paper, we explore the use of catecholate-to-iron(III) ligand-to-metal charge-transfer (LMCT) transitions as a probe of the iron coordination environment to complement the other techniques. Our series of synthetic catecholate complexes shows the effect of replacing ligands on the energy of the catecholate LMCT band, which reflects the Lewis acidity of the iron(III) center. These observations are then used to interpret the spectra of the catecholate complexes of phenylalanine hydroxylase and soybean lipoxygenase in their Fe(III) forms.

Experimental Section

Ligands. Catechol, 3,5-di-*tert*-butylcatechol, 3,4-dihydroxybenzoic acid, and 4-nitrocatechol were obtained from Aldrich. Catechol and 3,4-dihydroxybenzoic acid were sublimed under reduced pressure, 3,5-di-*tert*-butylcatechol was recrystallized from hexane before use, and 4-nitrocatechol was used without further purification. The methyl ester of 3,4,-dihydroxybenzoic acid (methyl protocatechuate) was obtained by the Fischer esterification of 3,4-dihydroxybenzoic acid.

The tripodal ligands used in this study are illustrated in Scheme I. NTA was used as received from Eastman Kodak. TPA·$HClO_4$[12] and NTB[13] were synthesized according to literature procedures. The identity of the products was confirmed by NMR spectroscopy. PDA was synthesized by a modification of the method of Harris et al.[14] Iminodiacetic acid (Aldrich; 6.55 g, 50 mmol) was added to a solution of 4.0 g (100 mmol) of NaOH in 20 mL of H_2O and 60 mL of absolute ethanol; the solution was stirred vigorously. Solutions of 8.2 g (50 mmol) of 2-picolyl chloride·HCl (Aldrich) in 17 mL of H_2O and 4.0 g (100 mmol) of NaOH in 7 mL of H_2O in separate addition funnels were then added over a period of 8 min. The reaction mixture was warmed to 70 °C and left to stir for 4 h. Then an additional 4.0 g of NaOH was added, and the reaction mixture was stirred for another hour, after which the amber solution was evaporated, leaving a yellow solid; 50 mL of H_2O was added and the solution acidified with concentrated HCl to pH 1.5. The white solid obtained was recrystallized from methanol; mp 184 °C dec; ^1H NMR in D_2O 3.81 (s, 4 H), 4.52 (s, 2 H), 7.73–7.80 (m, 2 H), 8.23–8.28 (m, 1 H), 8.68–8.70 (m, 1 H).

BPG was synthesized by the addition of 10 g (50 mmol) of bis-picolylamine (Nepara, Inc.) and 6.9 g (50 mmol) of bromoacetic acid (Aldrich) to 60 mL of absolute ethanol under N_2. Triethylamine (5.1 g, 50 mmol) was added and the solution refluxed overnight. The resulting solution was then cooled and the triethylammonium bromide removed by filtration. The solution was then chilled to 0 °C and diethyl ether was added to obtain a white solid, which was the expected product: mp 139–140 °C; ^1H NMR in D_2O 3.76 (s, 2 H), 4.44 (s, 4 H), 7.43–7.50 (m, 4 H), 7.88–7.93 (m, 2 H), 8.51–8.53 (m, 2 H).

Complexes. $(pyrrH)_2[Fe(HDA)DBC]$,[15] $(pyrrH)_2[Fe(Cl_2HDA)DBC]$, $(pyrrH)_2[Fe(Bu_2HDA)DBC]$, and $(pyrrH)_2[Fe(NTA)DBC]$ were synthesized according to published procedures.[16] (pipH)[Fe(PDA)DBC]·$0.5H_2O$ was synthesized by heating 250 mg (0.96 mmol) of PDA·HCl, 283 mg (0.96 mmol) of $FeBr_3$, and 0.473 mL (4.8 mmol) of piperidine in ethyl acetate under N_2 for 0.5 h; 213 mg (0.96 mmol) of DBC was then added under N_2 to form a dark blue-green solution, which was filtered hot. Upon cooling and standing overnight, the solution yielded fine needles. Anal. Calcd for $C_{29}H_{43}FeN_3O_{6.5}$: C, 58.69; H, 7.30; N, 7.08. Found: C, 58.65; H, 7.30; N, 6.96.

[Fe(BPG)DBC] was synthesized by heating 200 mg (0.78 mmol) of BPG and 314 mg (0.78 mmol) of $Fe(NO_3)_3·9H_2O$ in methanol under N_2. After 30 min, 173 mg (0.78 mmol) of DBC and 0.23 mL (2.34 mmol) of piperidine were added slowly under N_2. Crystals formed upon standing overnight. Anal. Calcd for $C_{28}H_{34}FeN_3O_4$: C, 63.16; H, 6.44; N, 7.89. Found: C, 62.98; H, 6.36; N, 7.72.

[Fe(NTB)DBC]$(NO_3)·H_2O$ was synthesized by heating 300 mg (0.74 mmol) of NTB and 298 mg (0.74 mmol) of $Fe(NO_3)_3·9H_2O$ in methanol under N_2. After 30 min, 164 mg (0.74 mmol) of DBC was added under N_2, and 0.146 mL (1.48 mmol) of piperidine was added slowly. Crystals were obtained by cooling overnight. These crystals were dried under vacuum before analyzing. Anal. Calcd for $C_{38}H_{43}FeN_8O_6$: C, 59.77; H, 5.68; N, 14.67. Found: C, 59.73; H, 5.57; N, 14.54.

[Fe(TPA)DBC](ClO_4) was synthesized by heating 150 mg (0.38 mmol) of TPA·$HClO_4$ and 155 mg (0.38 mmol) of $Fe(NO_3)_3·9H_2O$ in 25 mL of ethanol until dissolution, followed by the addition of 85 mg (0.38 mmol) of DBC and, finally, the slow addition of 0.15 mL (1.14 mmol) of piperidine to yield a green solution; 30 mL of degassed H_2O was then added to precipitate the complex. However, because of the extreme sensitivity of this complex to oxygen, it afforded a close but not satisfactory analysis.

Other catechol complexes were prepared in a similar manner to those above. The general procedure was to generate the iron–ligand complex anaerobically in the appropriate solvent, followed by the addition of the desired catechol along with the appropriate number of equivalents of base. The solutions yielded solids after concentration and cooling. Anal: $(pyrrH)_2[Fe(NTA)cat]$. Calcd for $C_{20}H_{30}FeN_3O_8$: C, 48.40; H, 6.09, N, 8.47. Found: C, 48.38; H, 6.16; N, 8.29. (pipH)[Fe(PDA)cat]·$0.33CH_3CN$. Calcd for $C_{21.67}H_{27}FeN_{3.33}O_6$: C, 53.57; H, 5.60; N, 9.60. Found: C, 53.91; H, 5.61; N, 9.33. [Fe(BPG)cat]·0.5DMF·$0.5H_2O$. Calcd for $C_{21.5}H_{22.5}FeN_{3.5}O_5$: C, 55.44; H, 4.87; N, 10.53. Found: C, 55.18; H, 4.52; N, 10.47. [Fe(NTB)cat](NO_3)·2DMF·$2H_2O$. Calcd for

(4) Que, L., Jr.; Heistand, R. H., II *J. Am. Chem. Soc.* **1979**, *101*, 2219–2221. Que, L., Jr.; Heistand, R. H., II; Mayer, R.; Roe, A. L. *Biochemistry* **1980**, *19*, 2588–2593.
(5) Tatsuno, Y.; Saeki, Y.; Iwaki, M.; Yagi, T.; Nozaki, M.; Kitagawa, T.; Otsuka, S. *J. Am. Chem. Soc.* **1978**, *100*, 4614–4615.
(6) Bradley, F. C.; Lindstedt, S.; Lipscomb, J. D.; Que, L., Jr.; Roe, A. L.; Rundgren, M. *J. Biol. Chem.* **1986**, *261*, 11693–11696.
(7) Que, L., Jr. *Coord. Chem. Rev.* **1983**, *50*, 73–108.
(8) Tatsuno, Y.; Saeki, Y.; Nozaki, M.; Otsuka, S.; Maeda, Y. *FEBS Lett.* **1980**, *112*, 83–85. Arciero, D. M.; Lipscomb, J. D.; Huynh, B. H.; Kent, T. A.; Munck, E. *J. Biol. Chem.* **1983**, *258*, 14981–14991.
(9) Wallick, D. E.; Bloom, L. M.; Gaffney, B. J.; Benkovic, S. J. *Biochemistry* **1984**, *23*, 1295–1302.
(10) Whittaker, J. W.; Solomon, E. I. *J. Am. Chem. Soc.* **1986**, *108*, 835–836.
(11) Arciero, D. M.; Lipscomb, J. D. *J. Biol. Chem.* **1986**, *261*, 2170–2178.
(12) Anderegg, G.; Wenk, F. *Helv. Chim. Acta* **1967**, *50*, 2330–2332.
(13) Thompson, L. K.; Ramaswamy, B. S.; Seymour, E. A. *Can. J. Chem.* **1977**, *55*, 878–888.
(14) Harris, W. R.; Motekaitis, R. J.; Martell, A. E. *Inorg. Chem.* **1975**, *14*, 974–978.
(15) Other abbreviations used: pyrr, pyrrolidine; $DBCH_2$, 3,5-di-*tert*-butylcatechol; $catH_2$, catechol; pip, piperidine; ehpg, ethylenebis(*o*-hydroxyphenylglycine).
(16) Que, L., Jr.; Kolanczyk, R. C.; White, L. S. *J. Am. Chem. Soc.* **1987**, *109*, 5373–5380.

Table I. EPR Data for [Fe(L)cat] Complexes[a]

complex	observed EPR g values	E/D
$[Fe(NTB)DBC]^+$	9.6, 4.3	0.33 (major, >90%)
	8.5, 5.5	0.13 (minor, <10%)
[Fe(BPG)DBC]	9.4, 5.1, 3.8, 3.5	0.22
$[Fe(PDA)DBC]^-$	9.4, 5.1, 3.8, 3.5	0.22
$[Fe(NTA)DBC]^{2-}$	8.7, 5.1, 3.5, 3.2	0.18
$[Fe(NTA)cat]^{2-}$	8.9, 5.0, 3.6, 3.3	0.20
$[Fe(HDA)DBC]^{2-}$	8.5, 5.3, 3.2, 2.8	0.15

[a] EPR spectra were obtained in DMF/Me_2SO/toluene glass at ca. 8 K. E/D values given are best matches to the second-order spin-Hamiltonian.

$C_{36}H_{43}FeN_{10}O_9$: C, 53.01; H, 5.31; N, 17.17. Found: C, 52.86; H, 5.27; N, 17.52.

Methods. Visible spectra were recorded on a Hewlett-Packard 8541A diode array spectrophotometer with values above 820 nm obtained on a Cary 219 UV–visible spectrophotometer. NMR spectra were recorded on a Bruker AC 300 spectrometer. EPR spectra were recorded at X band on a Varian E109 spectrometer fitted with an Oxford Instruments cryostat for measurements at liquid helium temperatures.

Resonance Raman spectra were obtained using Spectra-Physics Models 171 argon ion and 375B dye lasers. The spectra were recorded in 2-cm^{-1} steps using a Spex Industries Model 1403 spectrometer interfaced with a Spex Datamate. The solutions at millimolar concentrations were placed in a quartz spinning cell and collected at 90° with use of a constant slit width of 4 cm^{-1}. Features obtained in solution were referenced to the sulfate A_1 stretch at 983 cm^{-1} in aqueous solutions or a methanol-d_4 vibration at 985 cm^{-1}.

Biochemical Methods. Phenylalanine hydroxylase was isolated in the ferric form from the livers of retired male breeder rats by a modification[9] of the method of Shiman et al.[17] Saturating amounts of catechol were added to generate the catechol complex for spectroscopic studies. Visible spectra were obtained on a Cary 118 spectrophotometer.

Soybean lipoxygenase (isozyme-1) was purified by a modification of literature procedures.[18] The ferrous enzyme was oxidized by dilution of a concentrated solution of enzyme (60 mg/mL in 0.02 M potassium phosphate, pH 6.8) into two volumes of 0.1 M sodium borate, pH 9.0, and chilling to 5 °C. Aliquots of 10 mM linoleic acid (containing Tween 20 as dispersant) were added and an increase in intensity at 350 nm observed. At the initial appearance of intensity at 600 nm (indicative of an excess of hydroperoxide product), the sample was removed and dialyzed against 1500 volumes of 0.1 M potassium phosphate, pH 7.0, at 5 °C overnight. The sample of ferric lipoxygenase was removed and stored frozen at −20 °C.

Solutions of catechols were prepared anaerobically in 0.1 M potassium phosphate, pH 7.0. Visible spectra were recorded on a Perkin-Elmer Lambda 9 spectrophotometer in an anaerobic microcuvette chilled to 5 °C. Spectra were taken as the difference between those of the enzyme plus catechol and the enzyme alone. Aliquots of the catechol solution were added, and the spectral features were allowed to develop for 10 min. The titration was discontinued when no further increase in the intensity of the charge-transfer features was observed. EPR spectra were obtained using an IBM/Bruker ER/200 spectrometer equipped with an Air Products Helitran LTR-3 cryostat.

Results

A series of tripodal ligands, derivatives of trimethylamine, has been synthesized to provide a systematic variation on the ligand Lewis basicity in ternary complexes with Fe(III) and catechols. The structures of the ligands are shown in Scheme I, together with their abbreviations. The ternary complexes with 3,5-di-*tert*-butylcatechol, [Fe(L)DBC], have been synthesized and isolated as microcrystalline solids which afford satisfactory analyses. The corresponding catechol complexes have also been prepared; complexes of other substituted catecholates were generated in solution. The structure of the prototype complex of this series, $[Fe(NTA)DBC]^{2-}$, has been crystallographically determined;[16,19] NTA acts as a tetradentate ligand, and the catechol a bidentate ligand to yield a distorted octahedral complex. Similar structures are assumed for the other complexes in the series.

Table II. Catecholate Dependence of Absorption Maxima of [Fe(NTA)cat] Complexes in MeOH[a]

catecholate	λ_{max} (nm)
4-NO_2-cat	*396*, 490
3,4-dihydroxybenzaldehyde	400 (sh), 562
2,3-dihydroxybenzaldehyde	*354*, 578
methyl protocatechuate	382, 578
4-Cl-cat	398, 604
cat	410, 618
3-Me-cat	420, 634
4-Me-cat	418, 640
DBC	459, 682

[a] The numbers in italics are due to the transitions of the catechol itself. The higher energy charge transfer is obscured by these bands.

Table III. Absorption Maxima of LMCT Bands of Iron–Catecholate Complexes[a]

ligand	DBC	cat	methyl protocatechuate	4-NO_2-cat[b]
Bu_2HDA	435, 613	388, 550		
HDA	425, 643	400, 582		
Cl_2HDA	429, 666	404, 596		
NTA	459, 682	410, 618	382, 578	*396*, 490 (sh)
PDA	480, 732	426, 656	390, 596	*388*, 582
BPG	520, 788	460, 716	460, 662	*380*, 646
NTB	548, 842	490, 766	475, 718	*384*, 684
TPA	578, 888	495, 800		*366*, 722

[a] Data reported in nm obtained in methanol solvent. [b] The numbers in italics are due to the transitions of the catechol itself. The higher energy charge transfer is obscured by these bands.

Table IV. Solvent Dependence of Absorption Maxima of [Fe(L)DBC] Complexes

	NTA	PDA	BPG	NTB
DMF	414, 620	440, 682	488, 762	510, 816
CH_3CN	408, 622	444, 688	488, 764	528, 834
acetone		448, 696	490, 774	534, 858
CH_2Cl_2		478, 736	506, 794	542, 838
CH_3OH	459, 682	480, 732	520, 788	548, 842
n-C_4H_9OH	452, 684	478, 740	522, 808	558, 870

All the complexes in the series are ferric complexes, based on charge and stoichiometry. EPR spectra of several complexes, shown in Figure 1, indicate that these are all high-spin ferric. Analysis of the data (Table I) using the second-order spin-Hamiltonian for an $S = {}^5/_2$ system

$$\mathbf{H} = D[\mathbf{S}_z^2 - S(S+1)/3 + (E/D)(\mathbf{S}_x^2 - \mathbf{S}_y^2)]$$

shows that each complex exists as one major species (>90%). The E/D values obtained range from 0.15 for the trianionic HDA to 0.33 for the neutral NTB.

The complex $[Fe(NTB)DBC)]PF_6$, for example, exhibits a spectrum ($E/D = 1/3$) with peaks at $g = 9.5$ and 4.3, arising from the ground and middle Kramers doublets, respectively. The features are sharp ($\Delta H_{peak\text{-}to\text{-}peak}$ for the g 4.3 signal = 23 G) and rival those observed in proteins. Signals observed for proteins are usually sharper than those for synthetic complexes because of the greater homogeneity of the protein environment and the absence of solvent effects. Smaller features are observed at $g = 8.5$ and 5.5 arising from a minority species with $E/D = 0.13$; these account for less than 10% of the total spin concentration of the sample.[20]

The complex [Fe(BPG)DBC], on the other hand, exhibits signals at $g = 9.4$ (from the ground Kramers doublet) and 5.1, 3.8, and 3.5 (from the middle Kramers doublet) corresponding to $E/D = 0.21$. There is a small signal at $g = 4.3$ corresponding to a negligible amount of rhombic ferric impurity.[21] From a perusal of Table I, it is clear that the EPR parameters respond

(17) Shiman, R.; Gray, D. W.; Pater, A. *J. Biol. Chem.* **1979**, *254*, 11300–11306.
(18) Axelrod, B.; Cheesebrough, T. M.; Laakso, S. *Meth. Enzymol.* **1981**, *71*, 441–451.
(19) White, L. S.; Nilsson, L. H.; Pignolet, L. H.; Que, L., Jr. *J. Am. Chem. Soc.* **1982**, *104*, 2789–2796.
(20) Whittaker, J. W.; Lipscomb, J. D.; Kent, T. A.; Münck, E. *J. Biol. Chem.* **1984**, *259*, 4466–4475.
(21) The isotropic nature of the G = 4.3 signal leads to a large signal intensity relative to the other signals and accounts for its ready detection even when present in low levels (<1% of the total spin).

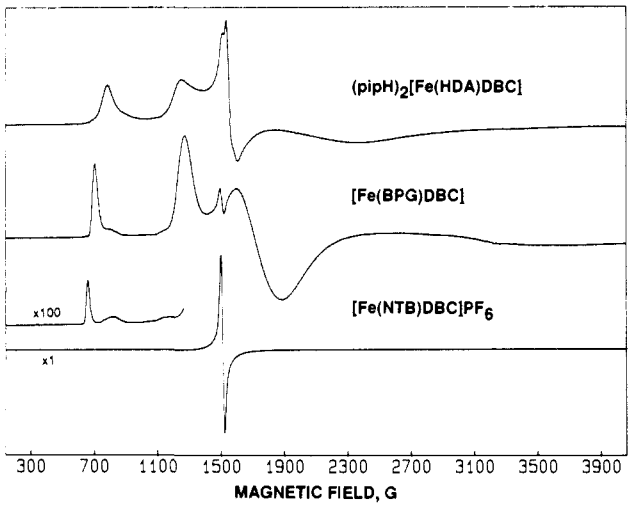

Figure 1. EPR spectra of (a) $(pipH)_2[Fe(HDA)DBC]$, (b) [Fe(BPG)-DBC], and (c) $[Fe(NTB)DBC]PF_6$, all dissolved in DMF/Me_2SO/toluene (2:1:2). Spectra at ca. 7 K were obtained at 9.24 GHz with 100-kHz modulation and a sweep width of 4000 G.

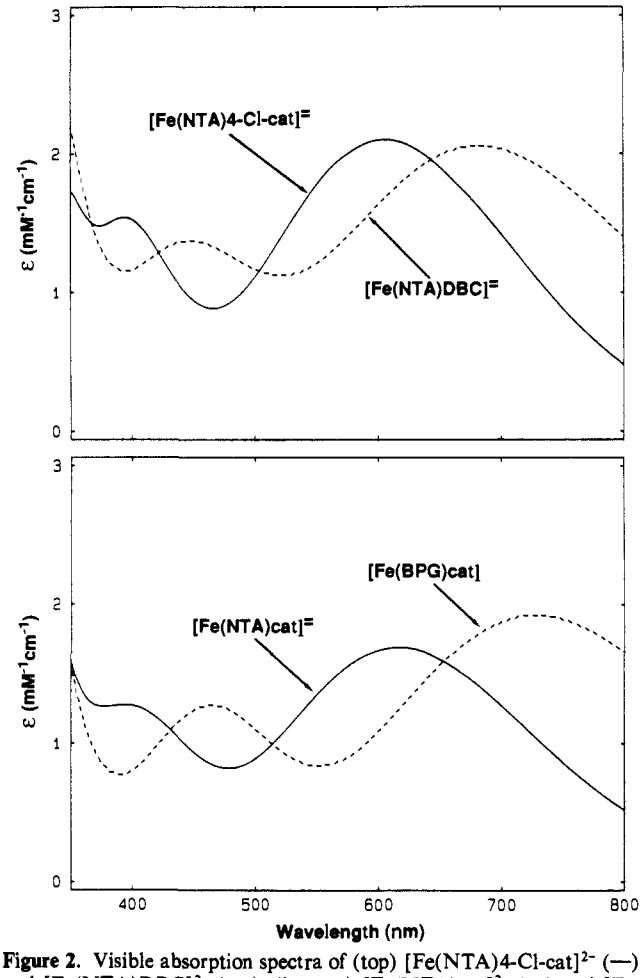

Figure 2. Visible absorption spectra of (top) $[Fe(NTA)4\text{-}Cl\text{-}cat]^{2-}$ (—) and $[Fe(NTA)DBC]^{2-}$ (---); (bottom) $[Fe(NTA)cat]^{2-}$ (—) and [Fe-(BPG)cat] (---). Spectra were obtained in methanol solution.

to changes in the metal environment; however, correlating the observed changes in E/D values with crystal-field symmetry and ligand-field strength will require further systematic studies.

The visible spectra of the [Fe(L)cat] complexes are dominated by two moderately intense absorption bands (Figure 2, Tables II–IV), similar to those observed in the spectra of iron phenolate[22]

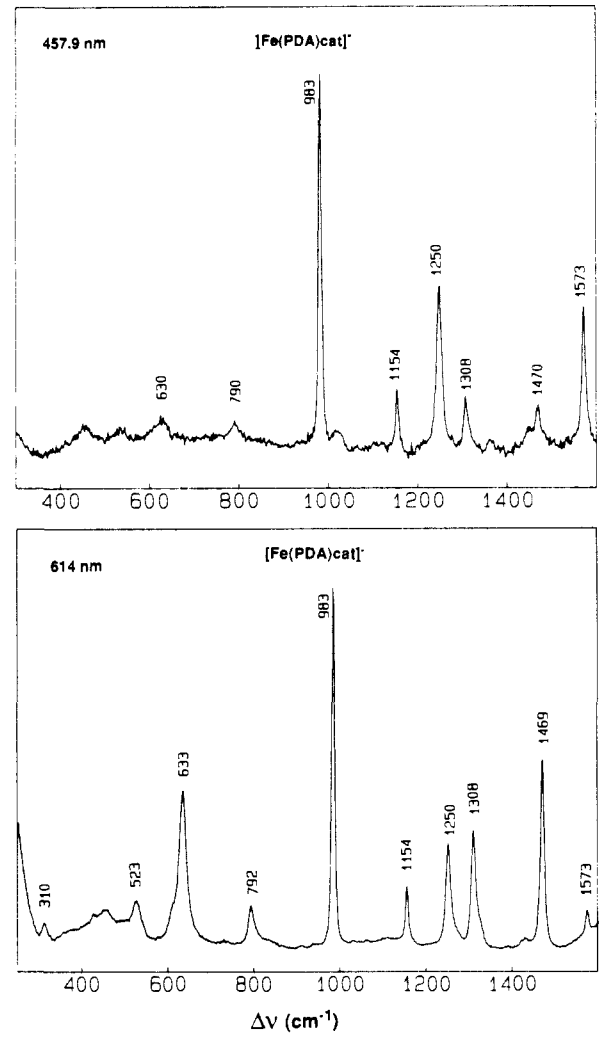

Figure 3. Resonance Raman spectra of $[Fe(PDA)cat]^-$. Conditions: 457.9 nm excitation (top) and 614 nm excitation (bottom), 120-mW power, 4-cm^{-1} slit width, ~1·mM complex in H_2O solvent with 0.1 M K_2SO_4 as internal standard.

and other iron catecholate complexes.[23,24] These bands are assigned as catecholate-to-Fe(III) charge-transfer transitions on the basis of resonance Raman experiments and the spectral shifts observed as the catecholate is varied.

The range of λ_{max}'s observed for the series of complexes allows both bands of certain complexes to be probed by the available laser lines for excitation. Raman spectra of $[Fe(PDA)cat]^-$ are shown in Figure 3. When probed with 614-nm excitation, $[Fe(PDA)cat]^-$ exhibits prominent features at 523, 633, 792, 1154, 1250, 1308, 1469, and 1573 cm^{-1}; all modes are affected by the deuteration of the catecholate ring protons and thus assigned to catecholate vibrations. The feature at 523 cm^{-1} is close to that assigned to the chelate ring mode at 528 cm^{-1} in $[Fe(oxalate)_3]^{3-}$ [25] and the 533-cm^{-1} peak in $[Fe(cat)_3]^{3-}$.[23] The features at 1154, 1250, 1469, and 1573 cm^{-1} are assigned to a C–H bend, a C–O stretch, and two C–C stretches, respectively, by analogy to deformations found in iron–phenolate complexes at ca. 1170, 1270, 1500, and 1600 cm^{-1}, respectively.[3,26] The 633- and 1308-cm^{-1} features may correspond to skeletal modes of ortho-disubstituted benzenes.[27] Similar spectra are observed for the other complexes

(22) Gaber, B. P.; Miskowski, V.; Spiro, T. G. *J. Am. Chem. Soc.* **1974**, *96*, 6868–6873.

(23) Salama, S.; Stong, J. D.; Neilands, J. B.; Spiro, T. G. *Biochemistry* **1978**, *17*, 3781–3785.

(24) Pyrz, J. W.; Roe, A. L.; Stern, L. J.; Que, L., Jr. *J. Am. Chem. Soc.* **1985**, *107*, 614–620.

(25) Nakamoto, K. *Infrared Spectra of Inorganic and Coordination Compounds*; Wiley-Interscience: New York, 1970; p 245.

(26) Tomimatsu, Y.; Kint, S.; Scherer, J. R. *Biochemistry* **1976**, *15*, 4918–4924.

Table V. Resonance Raman Spectra of Iron–Catecholate Complexes

complex	λ_{ex} (nm)	Raman vibrations (cm^{-1})							
Fe(NTB)cat]$^{+}$ [a]	605.1	518	630	828	1148	1248	1302	1454	1570
[Fe(BPG)cat][a]	613.5					1250	1306	1462	1574
[Fe(PDA)cat]$^{-}$ [b]	613.7	523	633	792	1154	1250	1308	1469	1573
[Fe(NTA)cat]$^{2-}$ [b]	514.5	526	630	794	1154	1254	1312	1473	1573
[Fe(salen)cat]$^{-}$ [c,d]	647.1	511	614	791	1145	1260	1324	1473	1560
[Fe(cat)$_3$]$^{3-}$ [b,e]	496.5	533	621	800	1154	1262	1322	1487	1572

[a] CD_3OD, bands referenced to solvent band at 1134 cm^{-1}. [b] H_2O, values referenced to SO_4^{2-} at 983 cm^{-1}. [c] CD_3CN, values referenced to solvent band at 1102 cm^{-1}. [d] Reference 24. [e] Reference 23.

in this study upon laser excitation into the lower energy band (Table V). These also correspond to spectra observed for [Fe(cat)$_3$]$^{3-}$ and [Fe(salen)cat]$^{-}$, indicating that the analogous transition is being probed for each case.[23,24]

Excitation into the higher energy band of the complexes results in spectra which differ from those observed with lower energy excitation. When probed with 457.9-nm excitation, [Fe(PDA)cat]$^{-}$ exhibits features at similar energies as the 614-nm spectrum, but their relative intensities have changed. The 1250- and 1573-cm^{-1} peaks dominate the spectrum, while the 633- and 1469-cm^{-1} peaks, which are the most intense in the 613.7-nm spectrum, are considerably diminished in size. With [Fe(BPG)cat] and [Fe(NTB)cat]$^{+}$, where the higher energy LMCT bands are redshifted, the Raman spectra obtained with 457.9-nm excitation exhibit only the features at ca. 1250 and 1570 cm^{-1}. These complexes provide the first opportunity to probe the higher energy band in catecholate complexes, and it is clear from the data that the catecholate vibrations associated with the two LMCT bands differ. However, the assignments for these vibrations and their dependence on excitation wavelength will require a more detailed investigation.

Table II shows the dependence of the spectra on the nature of the catecholate in the [FeNTA(cat)]$^{2-}$ series and supports the assignment of the transitions as ligand-to-metal charge transfer (LMCT) in nature. The lower energy absorption band is observed to shift to higher energy as the substituents on the catecholate are varied from electron donating to electron withdrawing. Electron-donating substituents would be expected to raise the energy of the catecholate frontier orbitals and thus minimize the ligand-to-metal gap. The higher energy band also shows the same general trend, although the exact position of the band is sometimes difficult to determine because of the presence of intraligand transitions.

Table III shows that the energies of these bands also exhibit a marked dependence on the nature of the tetradentate ligand. In this series of tripodal ligands based on trimethylamine, the pendant functionalities vary from phenolate and carboxylate to pyridine and benzimidazole. This affords a set of ligands of varying Lewis basicities and charge, while retaining similar coordination geometries. The catecholate LMCT bands shift to lower energies as the pendant oxyanion ligands are replaced by softer nitrogen ligands. In the DBC series, the lower energy LMCT band ranges from 613 to 888 nm, while the higher energy LMCT band ranges from 435 to 578 nm; in both cases, an energy shift of >5000 cm^{-1} is observed. Similar energy shifts are observed for the catechol, the methyl protocatechuate, and the 4-nitrocatechol series.

Table IV lists the solvent dependence for the LMCT bands of the DBC complexes; for aprotic solvents, the more polar solvents give rise to the more blue-shifted bands, as expected for a situation in which the excited-state dipole differs markedly from that of the ground-state dipole.[28] Protic solvents do not follow this trend, presumably because of hydrogen bonding effects; however, butanol gives rise to spectra that are red-shifted relative to those in methanol, in accordance to its lower polarity. Interestingly, the λ_{max}'s observed in methanol most closely match those observed in CH_2Cl_2. The solvent dependence shifts the frequency of the lower energy LMCT band by 700–800 cm^{-1} for the NTB, BPG, and PDA complexes and 1500 cm^{-1} for the NTA complex.

Discussion

The catecholate complexes in this study exhibit two LMCT bands in the visible region arising from the catecholate ligand. This suggests, at first glance, that the bands may arise from transitions to the metal d_π and d_σ orbitals originating from the same ligand orbital, thus affording an estimate of the octahedral crystal field, Δ_o. Such a model has been proposed for the electronic spectral features of [Fe(cat)$_3$]$^{3-}$ [23] and [Fe(ehpg)]$^{-}$.[22] However, this appears not to be the case for the catecholate complexes under study here on the basis of several observations. Table III shows that the energy difference between the two bands in the catechol series is ca. 8000 cm^{-1}, while that for the DBC series is ca. 7000 cm^{-1}; these are values which are significantly smaller than that expected for Δ_o for high-spin ferric complexes (ca. 10000 cm^{-1}).[29] It might also be expected that the more electron donating DBC would give rise to the larger Δ_o value. Secondly, the two bands have comparable extinction coefficients, which would be unlikely if the two transitions originated from the same ligand orbital, because the metal acceptor orbitals are of different symmetry. Lastly, excitation into the two LMCT bands results in the enhancement of different Raman vibrations. Taken together, the data suggest that different ligand orbitals are involved in the two LMCT transitions. Qualitatively, these two ligand orbitals can probably be assigned to the catecholate oxygen lone pairs; one set perpendicular to the ring plane would have π symmetry and be conjugated to the aromatic π orbitals, while the other set would be in plane and have σ symmetry. The energy difference between the two LMCT bands would then reflect not only the crystal-field splitting of the ferric ion but also the gap between the two sets of oxygen lone pairs.

More important for the biochemical applications is the dependence of the LMCT band energies on the nature of the tripodal ligand; the LMCT bands redshift as the pendant oxyanionic groups are replaced by neutral nitrogen ligands. A recent study of the phenolate-to-Fe(III) charge-transfer band in a series of Fe(salen)X complexes showed that substitution of a less Lewis basic X resulted in a red shift of the salen LMCT band and a positive shift of the Fe(III)/(II) redox potential.[24] The phenolate-to-Fe(III) charge-transfer band is thus an indicator of the redox potential of the metal center. Using similar arguments, we interpret the spectral shifts in the catecholate complexes as arising from the modulation of the effective Lewis acidity of the ferric center by the tetradentate ligand. The more highly charged oxyanion ligands such as HDA interact more strongly with the high-spin ferric center, neutralizing its inherent Lewis acidity and raising the metal d orbital energy relative to the catecholate filled orbitals, giving rise to blue-shifted LMCT bands. Substituents on the phenolate in the HDA subseries effect expected shifts in the spectra as the basicity of the phenolate is modulated.[30] The neutral ligands such as NTB and TPA have weaker interactions with the metal center and thus result in complexes with smaller catecholate-to-metal

(27) Varsanyi, G.; Szoke, S. *Vibrational Spectra of Benzene Derivatives*; Academic Press: New York, 1961; p 71.

(28) Lever, A. B. P. *Inorganic Electronic Spectroscopy*, 2nd ed.; Elsevier: New York, 1974; pp 208–212.

(29) Gray, H. B.; Schugar, H. J. In *Inorganic Biochemistry*; Eichhorn, G. L., Ed.; Elsevier: New York, 1973; Vol. 1.

(30) Only the lower energy LMCT band can be attributed to the catecholate; the higher energy band is a composite of catecholate and phenolate LMCT features and thus is not useful as a spectroscopic probe.

energy gaps and red-shifted spectra. The differences in metal–ligand interactions are reflected in metal–ligand bond lengths; Fe(III)–oxyanion bond lengths range from 1.8 to 2.0 Å, while Fe(III)–nitrogen bond lengths are typically 2.1–2.3 Å. By analogy to the Fe(salen)X study, the catecholate-to-Fe(III) charge-transfer band would also be an indicator of the redox potential of the iron site; such information should be useful for deducing the role of the metal center in metallooxygenases.

Applications to Nonheme Iron Oxygenases

The sensitivity of the catecholate LMCT bands to the nature of iron coordination environment suggests that catechols may be useful as probes for nonheme iron oxygenases such as phenylalanine hydroxylase[9] and soybean lipoxygenase.[31] Both these enzymes have ferric forms that exhibit no visible chromophore; the yellow color noted for these is a result of tailing of near-UV absorption features. Catechol coordination to the ferric centers of these enzymes should result in the observation of LMCT spectra which reflect the Lewis acidity of the ferric centers and suggest the nature of the other ligands coordinated to the iron. The enzymes, of course, may impose structural constraints on the coordination geometries of the enzyme–catechol complexes and may result in shifts in the absorption maxima which are not mimicked by the synthetic complexes. Nevertheless, our observations afford a first approximation of the coordination environment of the active site iron.

Phenylalanine hydroxylase (PAH) catalyzes the hydroxylation of phenylalanine to tyrosine in concert with a pterin cofactor. The rat liver enzyme as isolated is catalytically inactive and contains a high-spin ferric center; reductive activation by 6-methyltetrahydropterin is required to elicit hydroxylase activity.[9] The enzyme as isolated exhibits an EPR spectrum with signals at $g = 6.7$ and 5.3, associated with an $S = {}^5/_2$ system with $E/D = 0.03$. The binding of catecholamines results in a downfield shift of the $g = 6.7$ signal to 7.0, indicative of an increase of E/D to 0.04.[32] The visible spectrum of the catechol complex, shown in Figure 4 (top), exhibits an absorption maximum at 700 nm (ϵ 1140 M^{-1} cm^{-1}/subunit) and a shoulder at 410 nm; the difference spectrum of the catechol complex vs. the native enzyme shows the higher energy LMCT as a distinct peak at 455 nm. Excitation (620.5 nm) into the lower energy absorption feature reveals a Raman spectrum with catecholate vibrations similar to those observed in synthetic complexes from excitation of the lower energy band (Figure 4 (bottom)). Observation of the feature at 520 cm^{-1} strongly suggests that the coordinated catecholate is chelated to the metal center. Comparisons with Tables II, III, and IV indicate that the spectrum of the PAH–catechol complex is rather similar to that of [Fe(BPG)cat], suggesting that the ferric center of PAH has a Lewis acidity similar to that found for the BPG complex.

Soybean lipoxygenase catalyzes the oxidation of linoleic acid by oxygen, transforming the 9,12-*cis*,*cis*-diene unit to a 9,11-*cis*,*trans*-diene-13*S*-hydroperoxide. As isolated, the enzyme is inactive and contains a single high-spin ferrous ion. Oxidation by the product hydroperoxide yields the active, yellow, high-spin ferric enzyme whose EPR spectrum indicates the presence of multiple forms, all with $E/D < 0.09$.[33] Addition of catechol to lipoxygenase at pH 7 results in the immediate reduction of the active-site iron, as monitored by EPR spectroscopy; however, the use of electron-withdrawing catechols affords relatively stable complexes that may be characterized spectroscopically. For example, the visible spectrum of the 4-nitrocatechol complex of ferric lipoxygenase has been reported to consist of absorption features at 385 and 650 nm;[34] in our hands, the complex prepared by adding an equivalent of 4-nitrocatechol to ferric lipoxygenase at pH 7.0 shows visible absorption bands at 395 and 630 nm.[35] The methyl

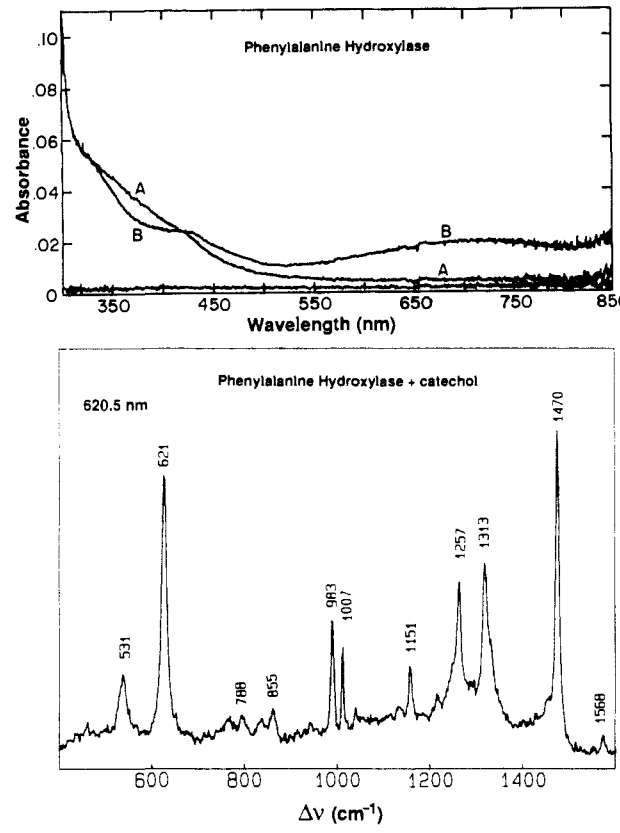

Figure 4. Top: Visible absorption spectra of (A) phenylalanine hydroxylase (17.5 μM enzyme in 50 mM Tris, pH 6.8) and (B) its complex with catechol (190 μM catechol added). Unlabeled spectrum is a baseline spectrum. Bottom: Resonance Raman spectrum of the complex of phenylalanine hydroxylase with catechol. Conditions: 620.5-nm excitation, 80-mW power, 4-cm^{-1} slit width, 1.1 mM enzyme with 1.8 mM catechol at 4 °C under N_2.

ester of protocatechuic acid also forms a complex with ferric lipoxygenase, yielding difference visible absorption bands at 455 and 670 nm (Figure 5). When correlated with Tables II–IV, the visible spectra most closely match to those of the corresponding Fe(BPG) complexes.

Our catechol probes into the active sites of phenylalanine hydroxylase and lipoxygenase indicate that both metal centers have Lewis acidities comparable to that of FeBPG. Because the carboxylate exerts the dominant effect on the Lewis acidity of the ferric center, our studies suggest that the iron coordination in both enzymes consists of a carboxylate ligand and three neutral ligands in addition to the catecholate. The neutral ligands would most likely be histidines, although methionine is also possible. The solvent dependence of the LMCT bands defines the margin of error for our conclusions. Since the two active sites are expected to be hydrophobic based on their substrate specificities, the values in CH_2Cl_2 would have been most appropriate for the comparison. We have used the values in methanol for comparison, because they nearly match those in CH_2Cl_2 (Table IV) and methanol dissolves all the complexes studied.

For phenylalanine hydroxylase, the proposed ligand set is consistent with the observed reduction of the ferric site by 6-methyltetrahydropterin ($E°$ = 250 mV vs. NHE).[36] For soybean lipoxygenase, the proposed ligand set is consistent with EXAFS estimates of three to four histidines coordinated to the iron[37] and would constitute only four of the six ligands on the six-coordinate site indicated by MCD studies of the Fe(II) enzyme.[10] Recent

(31) Veldink, G. A.; Vliegenthart, J. F. G. *Adv. Inorg. Biochem.* **1984**, *6*, 139–161.
(32) Bloom, L. M.; Benkovic, S. J.; Gaffney, B. J. *Biochemistry* **1986**, *25*, 4204–4210.
(33) Slappendel, S.; Veldink, G. A.; Vliegenthart, J. F. G.; Aasa, R.; Malmström, B. *Biochim. Biophys. Acta* **1981**, *667*, 77–86.
(34) Spaapen, L. J. M.; Verhagen, J.; Veldink, G. A.; Vliegenthart, J. F. G. *Biochim. Biophys. Acta* **1980**, *617*, 132–140.
(35) The difference may arise from the fact that the previous workers did not remove the products of the enzyme oxidation (presumably the 13-hydroxy-9,11-diene) before addition of catechol.
(36) Eberlein, G.; Bruice, T. C.; Lazarus, R. A.; Henrie, R.; Benkovic, S. J. *J. Am. Chem. Soc.* **1984**, *106*, 7916–7924.
(37) Feiters, M. C.; Vliegenthart, J. F. G.; Reedijk, J.; Malmström, B. G. *Recl. Trav. Chim. Pays-Bas* **1987**, *106*, 227.

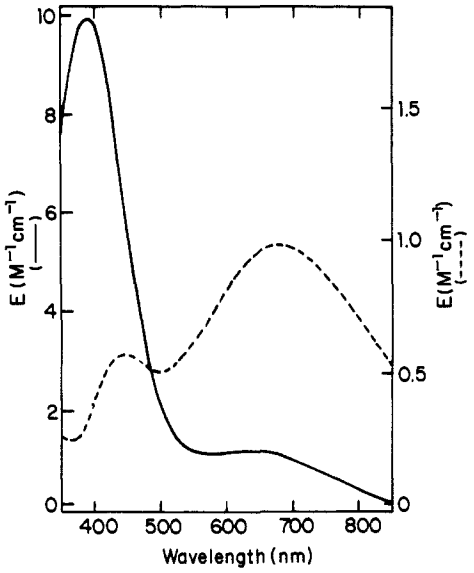

Figure 5. Difference visible absorption spectra of the complexes of soybean lipoxygen se with 4-nitrocatechol (—) and methyl protocatechuate (- - -) vs. oxidized lipoxygenase in 0.1 M potassium phosphate buffer pH 7.0 under N_2 at 5 °C.

EPR studies on the NO complex of Fe(II) lipoxygenase suggest that there is only one site for exogenous ligand binding;[38] upon binding, catechol probably occupies this exogenous ligand site and displaces an endogenous ligand as well. The endogenous ligands proposed for phenylalanine hydroxylase and soybean lipoxygenase are also those found in the active site of iron superoxide dismutase.[39,40] Such a ligand set would favor the Fe(II) oxidation state, yet still allow ready access to the Fe(III) state. In keeping with its function, the iron center of superoxide dismutase is well-poised electrochemically to be reduced by superoxide in the Fe(III) form and to be oxidized by superoxide in the Fe(II) form.

The roles of the metal centers of phenylalanine hydroxylase and lipoxygenase are not yet understood. For phenylalanine hydroxylase, the iron center may be the site for oxygen binding and its subsequent activation. The ligand environment may allow the iron center to shuttle between Fe(II) and Fe(IV) oxidation states for the hydroxylation reaction. Such a mechanism would differ from the formally Fe(III)/Fe(V) shuttle proposed for the cytochrome P450 mechanism.[41] For lipoxygenase, a current hypothesis for the enzyme mechanism involves deprotonation and oxidation of the 11-CH_2 of the 9,12-diene unit to yield an intermediate bis-allyl radical (or equivalent iron-coordinated species) that may then react with dioxygen.[42] The active site of lipoxygenase may have evolved so as to stabilize Fe(II), resulting in an Fe(III)/Fe(II) potential appropriate for the oxidation of the diene. The work reported here provides a starting point for elucidating the role of the metal in these oxygenation reactions.

Acknowledgment. This work has been supported by the National Institutes of Health (GM-33162, L.Q.) and the National Science Foundation (DMB-8316425, S.J.B.). We thank Dr. Eric Niederhoffer and Dr. James A. Fee for providing a sample of iron superoxide dismutase and Ms. Barbara Schuster for experimental assistance.

(38) Nelson, M. J. *J. Biol. Chem.* **1987**, *262*, 12137-12142.
(39) Ringe, D.; Petsko, G. A.; Yamakura, F.; Suzuki, K.; Ohmori, D. *Proc. Natl. Acad. Sci. U.S.A.* **1983**, *80*, 3879-3883. Stallings, W. C.; Powers, T. B.; Pattridge, K. A.; Fee, J. A.; Ludwig, M. L. *Ibid.* **1983**, *80*, 3884-3888. Stallings, W. C.; Pattridge, K. A.; Strong, R. K.; Ludwig, M. L. *J. Biol. Chem.* **1974**, *259*, 10695-10699.
(40) We have attempted the analogous catechol binding experiment with the iron superoxide dismutase from *E. coli* and were unable to form a complex. Dr. J. A. Fee (personal communication) has informed us that he was also unable to form the catechol complex. It is likely that catechol cannot gain access to the active site of superoxide dismutase because of the nature of the active site cleft. In contrast, both phenylalanine hydroxylase and lipoxygenase can accomodate the catechol presumably because of its similarity to the substrates.
(41) Ortiz de Montellano, P. R. In *Cytochrome P-450. Structure, Mechanism, and Biochemistry*; Ortiz de Montellano, P. R., Ed.; Plenum: New York, 1986; Chapter 7.
(42) Feiters, M. C.; Aasa, R.; Malmström, B.; Slappendel, S.; Veldink, G. A.; Vliegenthart, J. F. G. *Biochim. Biophys. Acta* **1985**, *831*, 302-305.

The Nature of the Phosphorus-Phosphorus Double Bond As Studied by Solid-State NMR

Kurt W. Zilm,*[1a] Gretchen G. Webb,[1a] Alan H. Cowley,[1b] Marek Pakulski,[1b] and Anita Orendt[1c]

Contribution from the Department of Chemistry, Yale University, New Haven, Connecticut 06511, and the Department of Chemistry, University of Texas at Austin, Austin, Texas 78712. *Received May 8, 1987*

Abstract: The nature of the P=P double bond in 1,2-bis(2,4,6-tri-*tert*-butylphenyl)diphosphene (**1**) has been studied by static and magic angle spinning ^{31}P solid state NMR. MAS spectra of **1** give an isotropic shift of +494 ppm relative to 85% orthophosphoric acid. Static powder spectra show an exceptionally large shift anisotropy with σ_{11} = 1236, σ_{22} = 249, and σ_{33} = −3 ppm. A two-dimensional NMR method has been applied which separates the dipolar coupling between the two ^{31}P nuclei from the chemical shift anisotropy and permits assignment of the orientation of the shift tensor in the molecular frame. The component at high field is approximately perpendicular to the CPP lane, and the low field component is in this plane and perpendicular to the direction of the phosphorus lone pair. By using the known bond length, the anisotropy in the indirect dipolar or scalar coupling between the two ^{31}P centers is also determined. These results are compared with the solid state spectra for 1,2-bis(2,4,6-tri-*tert*-butylphenyl)diphosphine (**2**) and 2,4,6-tri-*tert*-butylphenylphosphine (**3**). A comparison of these results with previous work on olefins and disilenes shows that the P=P double bond is similar in many respects to the double bonds formed by group IV elements.

Interest in multiply bonded compounds of the heavier main group elements has increased rapidly in the last 10 years as more and more examples of these species have been synthesized and characterized.[2] During this time the first examples of stable

0002-7863/88/1510-2032$01.50/0